



Article

Pathogenic Fungi Diversity of ‘CuiXiang’ Kiwifruit Black Spot Disease during Storage

Yaming Yang¹, Lijuan Chen^{1,2}, Chenyu Wang¹, Honghui Peng¹, Weijie Yin¹, Rui Li¹, Cuihua Liu¹, Xiaolin Ren^{1,*} and Yudian Ding^{1,*}

¹ College of Horticulture, Northwest Agricultural & Forestry University, Xianyang 712100, China; yangym@nwafu.edu.cn (Y.Y.); chenlijuan@nwafu.edu.cn (L.C.); wcy1004@nwafu.edu.cn (C.W.); penghonghui2021@163.com (H.P.); ywj2018050283@nwafu.edu.cn (W.Y.); lirui0410@nwafu.edu.cn (R.L.); liuch@nwafu.edu.cn (C.L.)

² Institute of Horticulture, Sichuan Academy of Agricultural Sciences, Chengdu 610000, China

* Correspondence: tjw689@126.com (X.R.); dingyudian@nwafu.edu.cn (Y.D.)

Abstract: Kiwifruit black spot disease has become increasingly widespread in many ‘CuiXiang’ kiwifruit plantings regions. This research was aimed at the pathogenic microorganisms of black spot of the ‘CuiXiang’ cultivar. Physiological, morphological and transcriptional characteristics between black spot fruit and healthy fruits were evaluated. Then, it applied a high-throughput internal transcribed spacer (ITS) sequencing to analyze the black spot disease microbial community. The cell structure showed that mycelium was attached to the surface of the kiwifruit through black spot, and that consequently the mitochondria were damaged, starch particles were reduced, and shelf life was shortened. Transcriptome revealed that different genes in kiwifruit with black spot disease were involved in cell wall modification, pathogen perception, and signal transduction. ITS sequencing results described the disease-causing fungi and found that the microbial diversity of black spot-diseased fruit was lower than that of healthy fruit. We predict that candidate pathogenic fungi *Cladosporium cladosporioides*, *Diaporthe phaseolorum*, *Alternaria alternata*, and *Trichothecium roseum* may cause black spot. This study was to explore the pathogenic fungal community of ‘CuiXiang’ kiwifruit black spot disease and to provide essential information for field prevention.

Keywords: black spot; ‘CuiXiang’; kiwifruit; internal transcribed spacer sequencing; transcriptome analysis



Citation: Yang, Y.; Chen, L.; Wang, C.; Peng, H.; Yin, W.; Li, R.; Liu, C.; Ren, X.; Ding, Y. Pathogenic Fungi Diversity of ‘CuiXiang’ Kiwifruit Black Spot Disease during Storage. *Horticulturae* **2022**, *8*, 13. <https://doi.org/10.3390/horticulturae8010013>

Academic Editors: Dong Zhang and Libo Xing

Received: 25 November 2021

Accepted: 20 December 2021

Published: 23 December 2021

Publisher’s Note: MDPI stays neutral with regard to jurisdictional claims in published maps and institutional affiliations.



Copyright: © 2021 by the authors. Licensee MDPI, Basel, Switzerland. This article is an open access article distributed under the terms and conditions of the Creative Commons Attribution (CC BY) license (<https://creativecommons.org/licenses/by/4.0/>).

1. Introduction

The kiwifruit (*Actinidia* spp.) is one of the important horticultural crops that is with rapidly grown in China [1]. China is rich in kiwifruit resources, planting area, and yield to reach the world’s demands [2]. ‘CuiXiang’ (*Actinidia deliciosa* ‘CuiXiang’) is a mid-early maturing cultivar with excellent fruit quality. ‘CuiXiang’ is very popular with consumers and is predominantly cultivated in China, particularly in Shaanxi province. ‘CuiXiang’ is a delicious early-maturing kiwifruit variety that has been selected and bred by Xi’an Kiwifruit Institute and Zhouzhi county’s Agricultural Technology Experimental Station, following more than 10 years of breeding work. *A. chinensis* is the paternal progenitor of *A. deliciosa* [3]. Black spot disease (also called blackhead, black mold, or mildew) has intensified on species of *Actinidia deliciosa*, especially ‘CuiXiang’. At the early stage (in June in Shaanxi), some small spots appear on the apex (stigma-end) of young fruits and become gradually contiguous. The disease only exhibits on the skin (outer pericarp) and cannot expand into the fruit pulp (mesocarp). The disease can accelerate the fruit’s softening and reduce the shelf life. In 2013, black spot disease appeared on ‘CuiXiang’ fruit [4]. At that time, the disease was regarded as being specific to ‘CuiXiang’. However, in 2019, ‘XuXiang’ fruit was found to have similar symptoms to ‘CuiXiang’ black spot disease [5]. Black spot disease damages the kiwifruit appearance and reduces the postharvest quality of fruits. It severely affects fruit quality and profitability.

Many researchers have different opinions on the pathogens of kiwifruit black spot disease. Fu et al. studied the pathogen of ‘CuiXiang’ black spot disease and preliminary concluded that the pathogen was *Diaporthe eres* [6]. Wang et al. isolated pathogenic fungi from diseased kiwifruit, and identified 99% homology with *Cladosporium* [7]. In addition, similar phenotypes of fruit black spot have been found in other kiwifruit cultivars [8–11], and it is worth noting that those phenotypes were different from that of ‘CuiXiang’ black spot disease in Shaanxi province. The pathogen of ‘CuiXiang’ kiwifruit black spot disease is still unclarified. We suspected that pathogenic microorganisms were difficult to cultivate in the laboratory, or that the cause of kiwifruit black spot disease required a comprehensive assessment of the multiple microorganisms interactions.

Metagenomics is an effective method to study microbial diversity. A primary metagenomic strategy for studying fungi is the ITS (internal transcribed spacer) sequence of fungi diversity. The ITS sequence is located in the region between 18S rDNA, 5.8S rDNA and 28S rDNA; it is highly conserved in the intraspecific level, and is diverse in the interspecific level, which is well used for classification identification and phylogenetic work of fungi [12]. Metagenomic methods can study and analyze the species composition, abundance and dominant bacteria of microorganisms [13]. At present, metagenome-based microbial sequencing technology has been successfully applied to study the postharvest microbial community of plum, apple, pear, and other fruits, so it is feasible to study the postharvest pathology of kiwifruit [14–16]. There are some studies on kiwifruit that have already carried out this methodology as well. For instance, Li et al. (DOI:10.1111/jph.12618) [17]. It is feasible to study the postharvest pathology of kiwifruit.

In this study, full-length amplification of ITS PacBio sequencing was used to comprehensively analyze the fungal diversity of ‘CuiXiang’ black spot disease and predict the main pathogenic microorganisms. It laid foundations for the isolation and verification of the pathogen and the comprehensive prevention and control of the disease.

2. Materials and Methods

2.1. Materials

Healthy and black spot disease infected fruits of ‘CuiXiang’ kiwifruit were harvested in September 2019, from five orchards (>5 years-old trees) in Yangling, Shaanxi Province (108.72 E, 34.36 N). Fruits were harvested at commercial maturity stage (average soluble solid content (SSC) was 7.5%). They were immediately transported to the laboratory and retained overnight to allow for wound healing and heat dissipation. Uniform and standard-shaped fruits without mechanical damage were selected and stored at the condition of room temperature 25 ± 2 °C and relative humidity (RH) $65 \pm 5\%$.

2.2. Measurement of Physiological Characteristics Data

2.2.1. Determination of Kiwifruit Firmness

Refer to the method of Barboni et al. [18] and make some improvements. A total of nine fruits were selected in each repetition. Peel small pieces of each fruit at the equator and measure twice. The two measurement positions should be kept perpendicular to each other, unit: N.

2.2.2. Kiwifruit Ethylene Production Rate

Refer to the method of Park et al. [19] and make some improvements. Place 12 fresh fruits in groups of 4 in 3 dryers. After keeping the sealed state for 1 h, use a 10 mL syringe to extract the gas in the tank and inject it into the vial underwater for sealing. A total of three gas extraction. Finally, the content of ethylene was determined by Trace GC Ultra ($\mu\text{L}\cdot\text{kg}^{-1}\cdot\text{H}^{-1}$). The carrier gas is 99.99% nitrogen, column temperature 70 °C, injector temperature 100 °C, and the temperature was 150 °C.

2.2.3. Determination of Soluble Solid Content and Titratable Acid Content

Extract the mesocarp (pulp) from the stalk and calyx of each fruit. The SSC was determined by the integrated sugar and acid analyzer, and the acid content was determined by diluting 200 μ L pure juice 50 times (unit: %).

2.2.4. Determination of Mineral Element Content

The content of acid-soluble calcium was slightly improved by referring to the methods of Shahkoomahally et al. [20] and Da Silva et al. [21]. The pulp of seriously ill, mildly ill, and healthy fruits were weighed and placed on tinfoil paper, and dried at 105 °C for 30 min, then dried at 70 °C until constant weight. Weigh 0.2 g of dried sample into sterilization tube, add 4mL nitric acid and 1ml hydrogen peroxide. The remaining liquid (MA165-001 Multiprep-41 FC2) after microwaving shall be diluted to 50mL for a certain number of times during testing. Calcium was determined by atomic absorption spectrometer (ZA3000). At the same time, water-soluble mineral elements were determined. Weigh 1 g frozen sample, add 10 mL pure water, shake well, centrifugal filtration. Finally, the volume was fixed to 10 mL, and the measurement was carried out on the machine.

The above measurements were repeated three times. Duncan's Range Multiple of ANOVA was used for significance test ($p < 0.05$ significant difference).

2.3. Observation of Scanning Electron Microscopy and Transmission Electron Microscope

2.3.1. Paraffin Sectioning

The peel tissues of diseased fruits and healthy fruits were cut into 0.5 cubic centimeters and fixed in FAA (Formalin–acetic acid–alcohol) fixating solution for more than 24 h. After this followed dehydration, transparency, wax-immersion embedding, slicing, staining, and sealing. The peel was observed with Olympus, U-TV0.63x optical microscope and photographed digitally.

2.3.2. Scanning Electron Microscopy Observation

The outer pericarps (exocarp skin) of diseased and healthy kiwifruits were cut into 1.0–1.5 cm² pieces, completely immersed in 4% glutaraldehyde fixing solution, and fixed at 4 °C for more than 6 h. It was rinsed in PBS (0.1 mol L⁻¹ Phosphate-buffered saline) three times, each time for 5–10 min, followed by stepwise 10%, 30%, 50%, 70%, 80%, 90%, 95%, and 100% alcohol concentration dehydration for 10–20 min. Next, it was dealcoholized for 15 min each in 25%, 50%, and 75% tert-Butanol concentration solutions, and then pure tert-Butanol for 30–40 min. The dry sample was placed in the sample stage, gold was sprayed in a vacuum sprayer, and it was observed and digitally photographed under an S-3400N electron microscope (Hitachi S-3400N, Hitachi, Tokyo, Japan) [22].

2.3.3. Transmission Electron Microscope Observation

The outer pericarps of healthy and diseased fruits were cut into 1 mm² pieces and fixed with 4% glutaraldehyde fixing solution (pH 6.8) at 4 °C for 14 h. After rinsing, post fixation, rinsing, dehydration, infiltration, embedding, cultured, sectioning, and dyeing, the pieces were observed and photographed under transmission electron microscope (JEM-1230, JEOL, Tokyo, Japan).

2.4. RNA Sequencing of Pulp Tissues during Storage

The RNA of pulp tissues was extracted from the healthy and diseased 'CuiXiang' during storage periods (0 and 5 DAH (days after harvesting), stored at room temperature 25 \pm 2 °C and RH 65 \pm 5%). A total of 1 μ g of RNA per sample was used as input material for the RNA sample preparation. After constructing the library, the samples were sequenced on an Illumina HiSeq platform by the Novogene Co. (Beijing, China). The Qubit 2.0 fluorometer was used for preliminary quantification, and then the Agilent 2100 bioanalyzer (Agilent Technologies, Palo Alto, CA, USA) was used to detect the insert size of the library to ensure quality. Illumina RNA sequencing was carried out to obtain

the reads. HISAT2 v2.0.5 was used to build an index of the reference genome and compare it with the reference genome. The gene expression levels were analyzed using the HTSeq v0.9.1 tool and expressed using the FPKM value (fragments per kilobase of transcript per million mapped reads). A total of three biological samples were used in each stage.

In order to identify the differentially expressed genes of kiwifruit with black spot during postharvest, transcriptome analysis was carried out on RNA-seq of fruit samples. The different expression genes (DEG) between healthy and diseased fruit samples were detected. A total of 1143 and 8805 DEGs detected that compared with healthy fruits were harvested at 0 and 5 DAH.

2.5. ITS Sequence and Bioinformatics Analysis of Fungal Communities on Fruit Surface

Healthy and diseased 'CuiXiang' kiwifruits were immersed in 0.5 L of 1% (*w/v*) peptone water and 1% (*v/v*) Tween-80 was added with a sterile beaker [23]. Then the Erlenmeyer flask was vigorously shaken for approximately 20 min to thoroughly wash the surface of the fruits. The suspension was filtered over a sterile polycarbonate membrane (0.22 μm pore size) held in a sterilized filtration device. The membrane containing the fungal filtrate was placed in a sterile tube and stored at $-80\text{ }^{\circ}\text{C}$ until the DNA extraction stage. Then the extracts underwent sequencing analysis (Novogene Bioinformatics Institute, Beijing, China) [24]. The experiment consisted of five separate biological replications from 5 orchards.

ITS sequences were detected by three-generation full-length amplicon sequencing technology. The species and abundance of fungi in 5 pairs of diseased and healthy tissue samples were analyzed. The raw ITS rDNA gene sequencing reads were demultiplexed and quality filtered by CCS (generate highly accurate single-molecule consensus reads) (SMRT Link v7.0) to correct the sequence with the following criteria: (1) the correction parameters were $\text{CCS} = 3$ and the minimum accuracy rate was 0.99 [25], (2) the shortest < 500 and the longest sequences length > 1000 were removed, (3) SSR (simple sequence repeat) filtering and Cutadapt (version 1.14) were used to remove the primers and filter out sequences containing consecutive identical bases > 8 , and (4) the result was compared with the full-length annotation database to remove chimera.

We assigned sequences with $\geq 97\%$ similarity to the same operational taxonomic units (OTUs) in UPARSE (Uparse v7.0.1001) [26] and then selected the sequences with the highest frequency of OTUs as the representative sequence. BLAST [27] in Qiime (Version 1.9.1) and the Unit Database (<https://unite.ut.ee/>, accessed on 23 March 2020) were used for species annotation analysis, and the community composition of each sample was counted at each classification level: boundary, phylum, outline, order, family, genus, and species. MUSCLE (Version 3.8.31) was used for fast multi-sequence alignment to obtain the systematic occurrence of all OTU representative sequences. Finally, the data of each sample were made uniform. Alpha and beta diversity analyses were based on the data after homogenization. We used Qiime (Version 1.9.1) to calculate Good's coverage indexes. R (Version 2.15.3), LEfSe, and Qiime (Version 1.9.1) were used to analyze the differences in diversity indexes. Unweighted UniFrac distance, principal component analysis, Chao1 index, Shannon index, and Venn diagram analysis were performed for OTU obtained by sequencing of healthy tissue and diseased fruit tissue. Fungal community diversity in healthy and diseased tissues was analyzed at phylum and genus levels.

Text mining work were carried out for search information of the significant fungi. Literature was retrieved from research articles in the NCBI PubMed and Web of Science databases. Information was screened for pathogenic fungi and antagonistic fungi related to plant diseases, and information on reducing their pathogenic association with black spot disease in kiwifruit. Text mining results of the pathogenicity of the significant fungi are listed in Table S1.

2.6. Laboratory Isolation, Purification, Identification, and Inoculation of Pathogenic Fungi

2.6.1. Isolation, Purification, and Identification of Pathogenic Fungus

The fruit surface was disinfected with 75% alcohol for 3–5 s, rinsed with distilled water and dried slightly. The peel at the junction of the fruit disease spots was removed on the very clean workbench and then placed in potato glucose agar medium (PDA), and cultured at 25 °C for 5–7 days. After growing hyphae, a very small number of hyphae at the edge of the colony was removed for separation and purification, and, after purification 5–6 times, samples for sequencing and identification were sent. The sequencing results of the isolated and purified 7 strains were compared with the existing ITS database BLAST.

2.6.2. Inoculation of Pathogenic Fungus

The cultured mycelium was scraped with a sterile knife, diluted and filtered with sterile water. Then the number of spores under the blood cell counting plate were observed. On the day of inoculation, the sample was diluted with sterile water into 1X10⁵ spore suspension/mL for standby. The surface of the healthy fruit was disinfected, and the outer skin layer of the kiwifruit was pricked with an inoculation needle μ L and then the spore suspension was dropped at the small hole and inoculated with sterile water as a control. A layer of polyethylene plastic film (0.01 mm thick) on the back cover was slightly dried to retain moisture. The sample was stored at room temperature (22 \pm 2 °C) and relative humidity of 85–90%. After inoculation for 15 days, the incidence of fruit was observed and counted. Duncan's Range Multiple of ANOVA was used for significance test ($p < 0.05$ significant difference).

3. Results and Discussion

3.1. Black Spot Disease Symptom during Postharvest: Accelerating Softening of Fruit, Visioning Hyphae Attached to Fruit Skin and Exhibiting Cell Wall Structure Changes

The kiwifruit stored at room temperature showed that black spot disease accelerated fruit softening (Figure S1). The physiological indexes of kiwifruit diseased fruit (with different degree of disease) and healthy fruit were preliminarily detected under normal temperature storage. Results showed the black spot could significantly affect the firmness of fruit, accelerate ethylene production, and significantly shorten the shelf life. The SSC of black spot kiwifruit was higher than healthy fruit, and the content of water-soluble calcium was significantly lower than that of healthy fruit (Figure S2). The taste of kiwifruit can be affected by a number of components, including SSC and TA [18]. The mineral composition of kiwifruit is an important factor for its nutritional quality, in particular its nutritional properties (sodium/potassium ratio) [28]. Preharvest treatment of Ca-chitosan delayed the loss of firmness in kiwifruit during cold storage [29]. Therefore, the measurement of these physiological characteristics can explain the impact of black spot disease on 'CuiXiang' kiwifruit.

The microscopic aspects illustrated the difference between healthy and diseased fruit at the cell microstructure level. On the surface of diseased kiwifruit skins were scattered black spots (Figure 1A). Paraffin section observation showed that the keratinocytes of the diseased fruit were thicker than those of the healthy fruit, and the epidermal cells of the healthy fruit were arranged more orderly (Figure 1B). The results of transmission electron microscope showed that relatively complete cells, including mitochondria, starch granules and other organelles, could be observed in the healthy pericarp, and a relatively obvious bright–dark–bright zoning structure could be seen, while the mitochondria, starch granules, and other organelles in the diseased pericarp were damaged (Figure 1C). It was also observed by scanning electron microscopy that the diseased peels showed filaments resembling mycelium, with different shapes. Some were a cluster of round ovate shapes, and some were elongated and cylindrical, growing from the epidermal tissue of the peel. The healthy peel had less filamentous material and a smooth surface. Scanning electron microscope results showed that there were hyphae on the surface of the diseased fruit (Figure 1D).

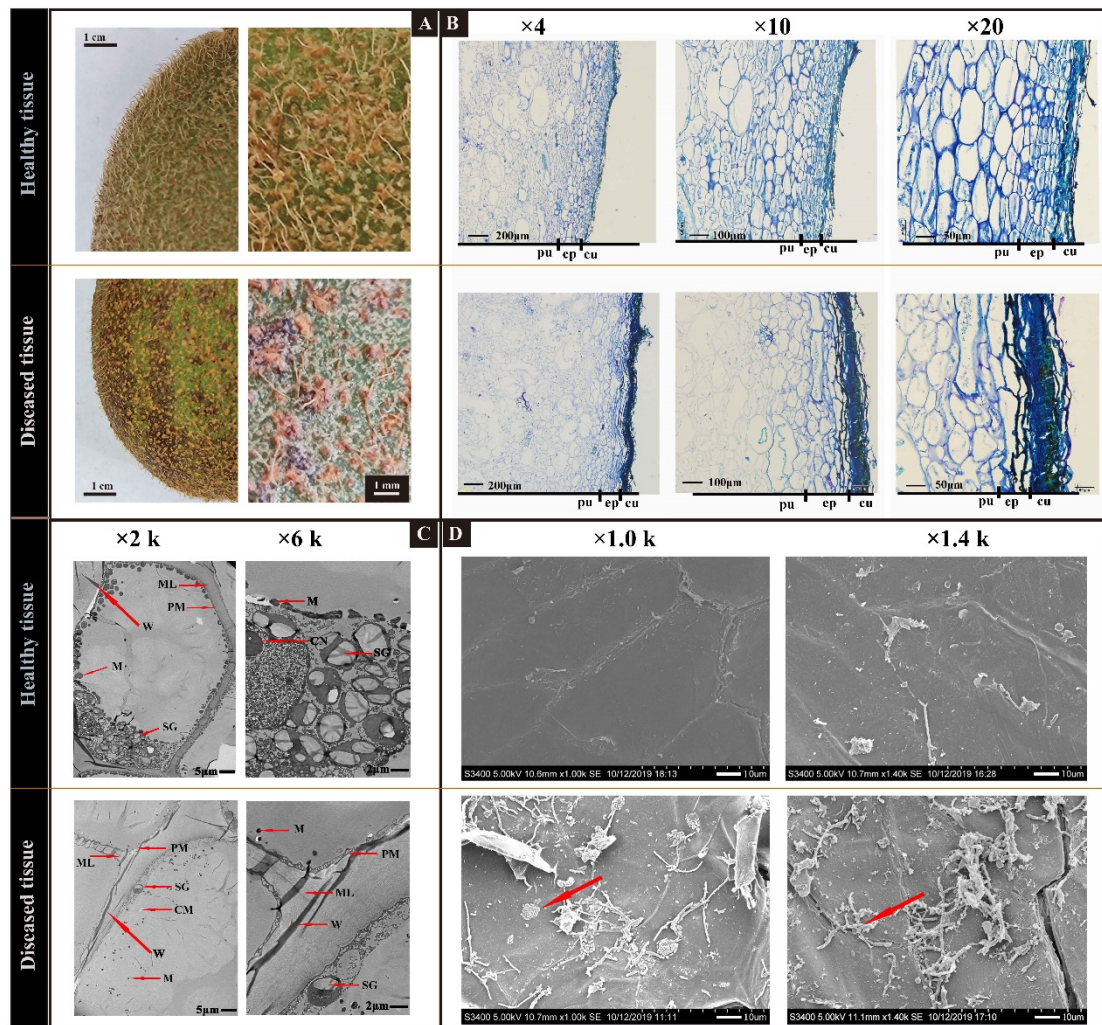


Figure 1. Phenomena of ‘CuiXiang’ healthy fruit and black spot diseased fruit. (A) The surface of diseased and healthy kiwifruit. (B) Paraffin sections of outer pericarps of healthy and diseased fruits. The equatorial pericarp of healthy and diseased fruit was fixed, dehydrated, wax-soaked and embedded, sliced, stained and sealed, and finally observed and photographed by a positive fluorescence microscope at Olympus BX51 (cu-cuticle, ep-epidermal cells, pu-pulp cells, SG-starch granule; magnification times: $\times 4$, $\times 10$ and $\times 20$). (C) Transmission electron microscope observation of pericarp of healthy and diseased fruits. Note: ML-medium adhesive layer; M-mitochondria; CM-vacuolated mitochondria; PM-plasma membrane; SG-starch grain; W-wrinkle. (D) Scanning electron microscope observation of healthy and diseased fruit surface. Healthy and diseased fruit peel were cut into 1.0–1.5 cm² pieces and observed under an S-3400N electron microscope (acceleration voltage: 5.00 kv, mm: the distance of the sample from the probe, magnification times: $\times 1.00\text{ k}$ and $\times 1.40\text{ k}$).

In summary, the phenomena of black spot disease symptom of kiwifruit indicated: (1) the thickness of cuticle and epidermal cells on fruit surface will affect its water loss [30], paraffin wax results show that the cuticle of healthy fruit is thinner than that of diseased fruit, which can explain the faster water loss of healthy fruit; (2) the degradation of the cell wall is considered to directly lead to fruit softening [31]; (3) scanning electron microscopy showed that hyphae attached to the host cell wall. The short shelf life of diseased fruit indicates that the pathogen invades the related enzymes that may be released from the host cell wall, resulting in the semi disintegration or complete disintegration of the organelles of the host cells; and (4) mitochondria are an important place for fruit aerobic respiration. The number and integrity of mitochondria affect the process of fruit senescence [32]. In this

study, compared with healthy fruit, the mitochondrial structure of diseased fruit was damaged, the number was significantly less, and the number of starch particles decreased and gradually weakened; the cell wall was severely deformed.

3.2. Transcription Influence of Black Spot Disease on Fruits: Cell Wall Modification and Pathogen Signals Genes Were Regulated

A total of 1143 and 8805 DEGs detected that compared with healthy fruits were harvested at 0 and 5 days after harvesting (DAH) (Figure 2A). In this study, DEG involved in cell wall modification was regulated to varying degrees in different storage periods (Figure 2B). Encoding, such as polygalacturonase (PG, Achn144331), xyloglucan endotransglucosylase (XTH, Achn088411), pectate lyase (PL, Achn070291 | Achn315151), and expansin (EXP, Achn382301), were up-regulated. The cell wall is the basic barrier of the plant defense system in response to pathogen attack [33]. Especially during fruit ripening, the disintegration of the cell wall allows pathogens to easily invade [34]. When plants are infected by pathogens, they will detect pathogen signals through pattern recognition receptors (PRRs) [35].

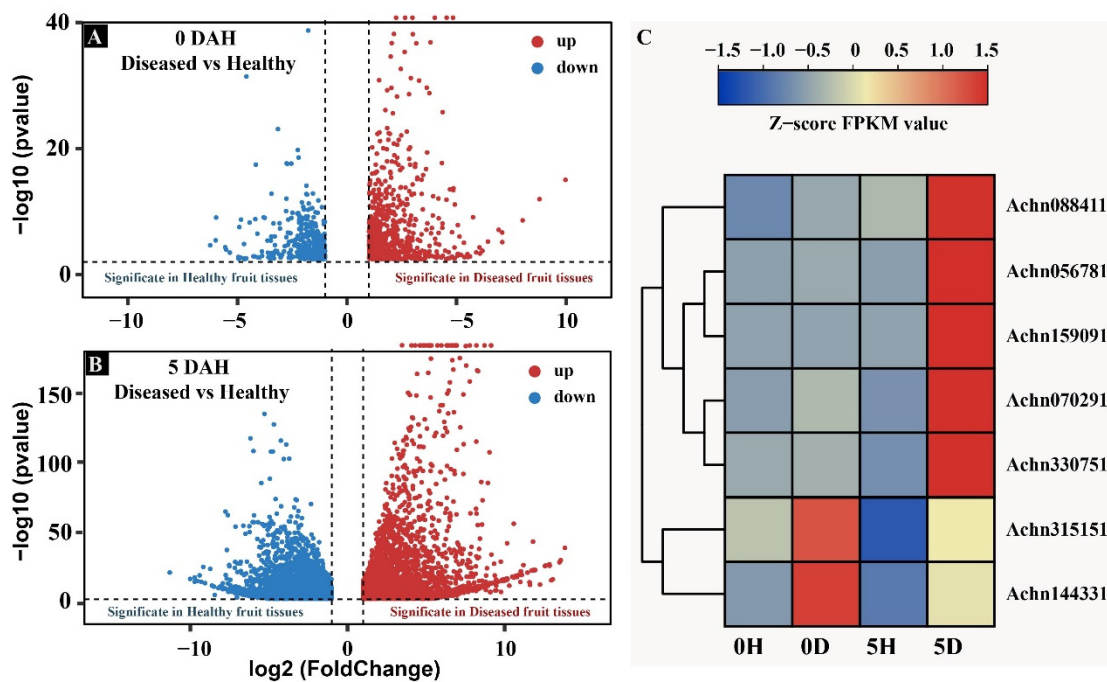


Figure 2. Transcriptome difference of healthy and diseased fruit after harvest. (A,B) The DEGs between healthy and diseased fruit pulps were assigned with a threshold of $|\log_2(\text{Fold Change})| > 1$ and $\text{padj} < 0.05$. A total of 1143 and 8805 DEGs were detected at 0 and 5 DAH. (C) Heatmap of DEGs involved in annotation of cell wall modification and pathogen signals. Encoding genes, such as polygalacturonase (PG, Achn144331), xyloglucan endotransglucosylase (XTH, Achn088411), pectate lyase (PL, Achn070291 | Achn315151), and expansin (EXP, Achn382301), were up-regulated. Some DEGs that involved in pathogen perception and signaling transduction of PRR genes were significantly induced after kiwifruit was infected with black spot disease. They included various types of receptor-like kinases (RLKs) and receptor-like proteins (RLPs), such as LRR receptor-like serine/threonine-protein kinase (Achn056781); receptor-like serine/threonine-protein kinase (Achn330751) and receptor-like protein kinase (Achn159091) were up-regulated.

Some DEGs involved in pathogen perception and signaling transduction of PRR genes were significantly induced after the kiwifruit was infected with black spot disease (Figure 2C). They included various types of receptor-like kinases (RLKs) and receptor-like proteins (RLPs), such as LRR receptor-like serine/threonine-protein kinase (Achn056781);

receptor-like serine/threonine-protein kinase (Achn330751) and receptor-like protein kinase (Achn159091) were up-regulated.

In summary, RNA-seq revealed the transcriptional response of black spot kiwifruit during postharvest storage. Most cell wall modification genes were up-regulated in diseased fruits, suggesting that black spot infection affects shelf life through cell wall related enzymes. At the same time, kiwifruit with black spot disease is also involved in pathogen perception and signal transduction.

3.3. OTU Statistical Analysis of Fungal Community: The Species and Abundance of Microorganisms of Healthy Fruit Tissues Were Higher than That of Diseased Tissues

ITS sequencing was performed to illuminate the fungal environment on fruit surfaces between diseased and health fruits. Sequencing results of fungi in five pairs of samples (from five orchards) showed that there were differences in fungal communities between healthy and diseased fruit surfaces. All 60,095 clean reads were clustered into operational taxonomic units (OTUs) with 97% identity, then were polymerized into 497 OTU sequences. Representing 497 different fungi, homogenization was performed with the least amount of sequence data. Finally, the OTU of the healthy fruit surface was 413, while that of diseased fruit was 271, suggesting that there were more fungal species on healthy fruit surface than infected fruit. The good coverage index showed that the sequences of all samples reached the saturation stage, and the coverage index was $\geq 97.70\%$ (Table 1).

Table 1. Summary of the ITS sequences of the fungal community samples.

Sample	Clean Reads	Total Bases	Average Length	Goods Coverage	OTU (97%) *
H1	5593	3,822,534	683	0.993	146
H2	6612	4,459,569	674	0.989	155
H3	5899	4,027,333	682	0.988	178
H4	6171	4,252,244	689	0.984	177
H5	5688	3,888,406	683	0.977	170
D1	6089	4,239,139	696	0.989	130
D2	5993	4,142,348	691	0.988	132
D3	6079	4,105,757	675	0.991	138
D4	5899	4,358,927	738	0.99	93
D5	6072	4,186,335	689	0.994	97
Average health	5992.6	4,090,017	682.2	0.9862	165.2
Average disease	6091.8	4,173,338	684.8	0.9854	162

* MUSCLE (Version 3.8.31) was used for fast multi-sequence alignment to obtain the systematic occurrence of all OTU representative sequences. OTUs are used to categorize fungi based on sequence similarity. In metagenomics approaches, OTUs are a cluster of similar sequence variants of the ITS marker gene sequence. Each of these cluster is intended to represent a taxonomic unit of a fungi species or genus depending on the sequence similarity threshold. Typically, OTU clusters are defined by a 97% identity threshold of the ITS gene sequences to distinguish fungi at the genus level.

According to the unweighted UniFrac heatmap and PCoA (principal co-ordinates analysis) map (Figure 3A,B), which reflected the beta diversity of fungal groups, there were significant differences in fungal communities between black spot diseased fruit and healthy fruit. UniFrac is a β -diversity measure that uses phylogenetic information to compare environmental samples. Beta diversity shows the difference between microbial communities from different environments. The main focus is on the difference in taxonomic abundance profiles from different samples. Unweighted UniFrac purely based on sequence distances does not include abundance information. Weighted UniFrac are weighted by relative abundances and includes both sequence and abundance information. UniFrac could couple with standard multivariate statistical techniques including principal coordinates analysis (PCoA), and identifies factors explaining differences among microbial communities. Healthy fruit and susceptible fruit were obviously divided into two different groups, which further explained the differences between healthy fruit and susceptible fruit groups.

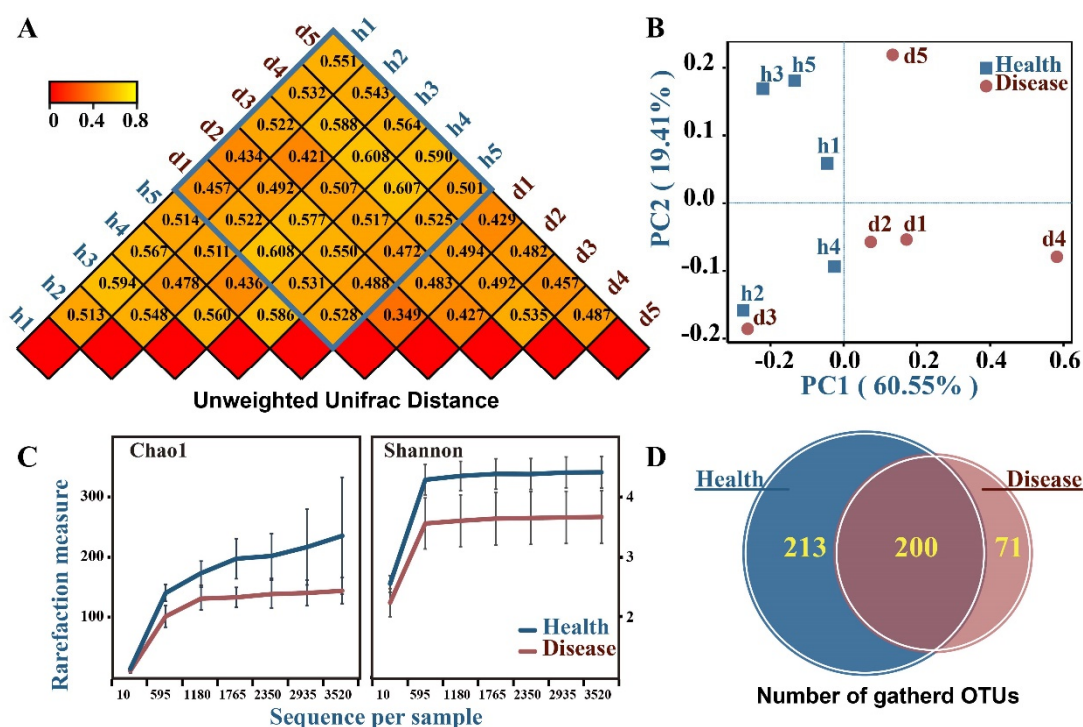


Figure 3. Variance analysis of fungal communities between healthy and diseased tissues. (A) Unweighted UniFrac distance of OTUs abundance between healthy and diseased tissues (samples from five orchards). (B) PCoA analysis based on UnWeighted UniFrac distance of OTUs abundance. UniFrac is a β -diversity measure that uses phylogenetic information to compare environmental samples. Beta diversity shows the difference between microbial communities from different environments. The main focus is on the difference in taxonomic abundance profiles from different samples. Unweighted UniFrac purely based on sequence distances does not include abundance information. Weighted UniFrac are weighted by relative abundances and includes both sequence and abundance information. UniFrac could couple with standard multivariate statistical techniques, including principal coordinates analysis (PCoA), and identifies factors explaining differences among microbial communities. (C) Alpha diversity analysis of samples. Alpha diversity summarizes the structure of an ecological community with respect to its richness (number of taxonomic groups) and evenness (distribution of abundances of the groups). The Chao1 index is a qualitative measure of alpha diversity which includes species richness. It returns an estimate of species richness based on a vector or matrix of abundance data. The Shannon index summarizes the diversity in the population while assuming all species are represented in a sample and that they are randomly sampled. The Shannon index increases as both the richness and evenness of the community increase. (D) Venn figure of OTU count in each group. There are 200 OTUs that are common to healthy fruits and diseased fruits, 213 OTUs solely in healthy fruits, and 71 OTUs only in diseased fruits. We focused on OTUs unique to healthy or diseased fruit.

According to alpha diversity index and Venn diagram (Figure 3C,D), which reflect fungal diversity, Chao1 index and Shannon index of healthy fruit were higher than those of diseased fruit, suggesting that the species and abundance of microorganisms on the healthy fruit surface were higher than that on the diseased fruit surface. The Chao1 index is a qualitative measure of alpha diversity which includes species richness. It returns an estimate of species richness based on a vector or matrix of abundance data. The Shannon index summarizes the diversity in the population while assuming all species are represented in a sample and that they are randomly sampled. The Shannon index increases as both the richness and evenness of the community increase. High diversity of microbial species contributes to maintaining a stable microbial environment on fruit surface [36,37]. Once that balance is broken, the number of pathogens that cause black spot increases dramatically.

There were 200 common OTUs on the surface of infected and healthy fruit, 213 OTUs were unique to the surface of healthy fruit, and 71 OTUs were unique to the surface of infected fruit. The OTU statistical analysis indicated that dominant and pathogenetic species existed in fungal communities of the diseased samples.

3.4. Prediction and Analysis of Pathogenic Fungi

Species annotation and relative abundance between disease and health tissues indicated candidate pathogenic fungi. Species annotation at phylum level show that fungi in healthy fruits are qualitatively similar to those in diseased fruits (Figure 4A). The relative abundance of Ascomycota in healthy fruit was higher than that in diseased fruit. The second class is unclassified fungi, comprising 28.20% of diseased fruit, which was higher than 21.60% of healthy fruit. The microbiome of healthy fruits mainly consists of Basidiomycota, Chytridiomycota, Monoblepharomycota, and Entomophthoromycota, and its relative abundance is also higher than that of black spot fruits. At the genus level, 35 genera with the greatest difference in fungal abundance in healthy tissues were noted (Figure 4B). Fungi belonging to *Tilletiopsis*, *Fusarium*, *Golubevia* and *Sarocladium* had high abundance in diseased fruits. Healthy fruit surface enriched to *Acremonium*, *Farysia*, *Cladosporium*, *Moesziomyces*, *Aureobasidium*, *Symmetrospora*, *Rhizophlyctis*, *Kondoa*, *Filobasidium*, *Erythrobasidium*, *Ciliophora*, *Gibberella*, *Acaromyces*, *Hanseniaspora*, *Phoma*, *Fusariella*, *Plectosphaerella*, *Vishniacozyma*, and *Gibellulopsis*.

Biomarkers with statistically significant differences between diseased and healthy fruit were searched by LDA Effect Size (LEfSe) (Figure 5A,B). At different levels of classification, fungi with significant differences between healthy and diseased fruit included C-Exobasidiomycetes, F-Golubeviaceae, O-Golubeviales, G-*Golubevia*, and *Golubevia* sp. (Figure 5C). These fungi may play important roles in diseased fruit.

Text mining work was carried out to search for the pathogenicity of the significant fungi (Table S1). Results showed that a variety of pathogenic and antibiogenic fungi had been reported related to plant pathogens, e.g., plant leaf spots and fruit rot. Previously, *Diaporthe eres* (sexual) or *Phomopsis* (monogenesis) [6], *Cladosporium* [7], *Didymella glomerata* [8], *Nigrospora oryzae* [9], *Alternaria alternata* [10], and *Pseudocercospora actinidiae* [11] have been reported to be associated with kiwifruit black disease. On the other hand, there were antagonistic species of pathogenic fungi with high abundance in healthy tissues, such as *Hanseniaspora uvarum*, *Acremonium sclerotigenum*, *Aureobasidium pullulans*, and *Acaromyces ingoldii*. These three species are known to play a role in bioantagonism [35,38–40]. *Acremonium sclerotigenum* is positive for the production of β -1-3 glucanase, cellulase, and compounds, which are involved in biocontrol mechanisms [38].

3.5. Identification of Pathogenic Fungus

A total of seven strains were isolated and purified from diseased fruit surface (Figure 6; Table S2). They were sequenced and BLAST annotated. Results showed that fungi strains of number (No.) 4, No. 7, and No. 8 were annotated as *Diaporthe eucalyptorum*, *Paraphaeosphaeria michotii* and *Fusarium nygamai*, respectively. Strains No. 1, No. 2, No.5 and No. 6 belong to neopestalotiopsis, *Fusarium*, *Epicoccum* and *Alternaria*. A total of seven kinds of fungi, distilled water and mixed fungal solution were inoculated into healthy 'CuiXiang' kiwifruit at 22 ± 2 °C. After 15 days, it can be observed that the part inoculated with sterile water has no rot or disease spots. The fruit spots inoculated with No. 1, No. 4, No. 5, No. 6, and No. 7 fungi showed leather shape, hard and no pathological changes in the pulp. The pulp of the fruit inoculated with strain No.2 appeared white, and the white hyphae on the peel of strain No. 2 were similar to strain No. 8. White hyphae also grew on the peel inoculated with mixed fungal solution, and the pulp rotted. It can be seen from Table S2 that the fruits inoculated with fungi show lesions to a certain extent, and the lesion diameter is significantly different under the inoculation of different strains, but it is not the disease of black spot. In conclusion, there was no symptom of black spot disease after inoculation with the seven isolated strains.

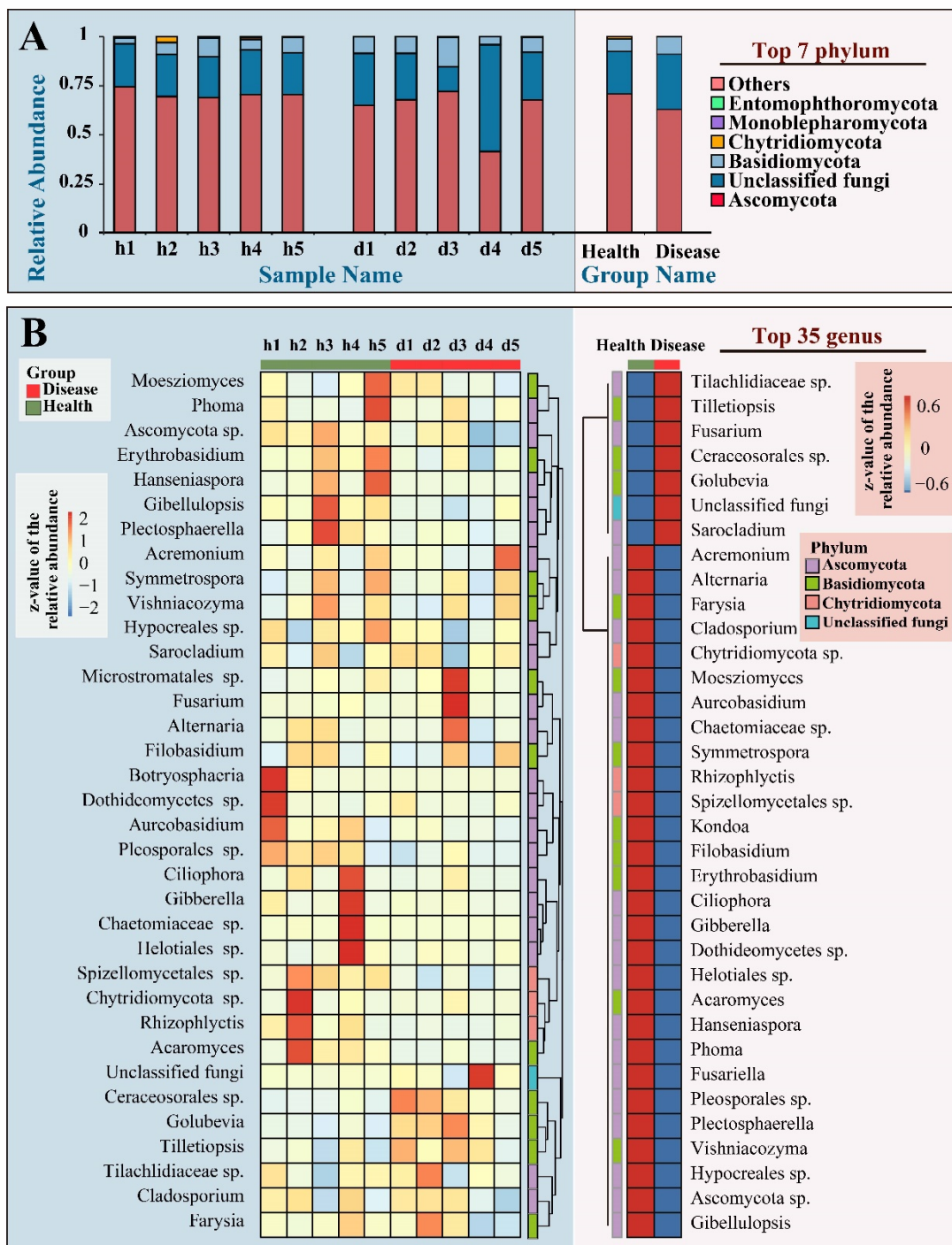


Figure 4. Diversity of fungal communities of healthy and diseased tissues at the phylum (A) and genus (B) level. (A) A histogram is illustrating diversity of fungal communities at phylum level. It shows relative abundance of top 7 phylum. (B) Histograms are illustrating diversity of fungal communities at genus level. It shows relative abundance of top 35 genera. The corresponding value of heat map is the z-value of the relative abundance. Class others represent the sum of the relative abundance of all OTUs except those listed in the figure.

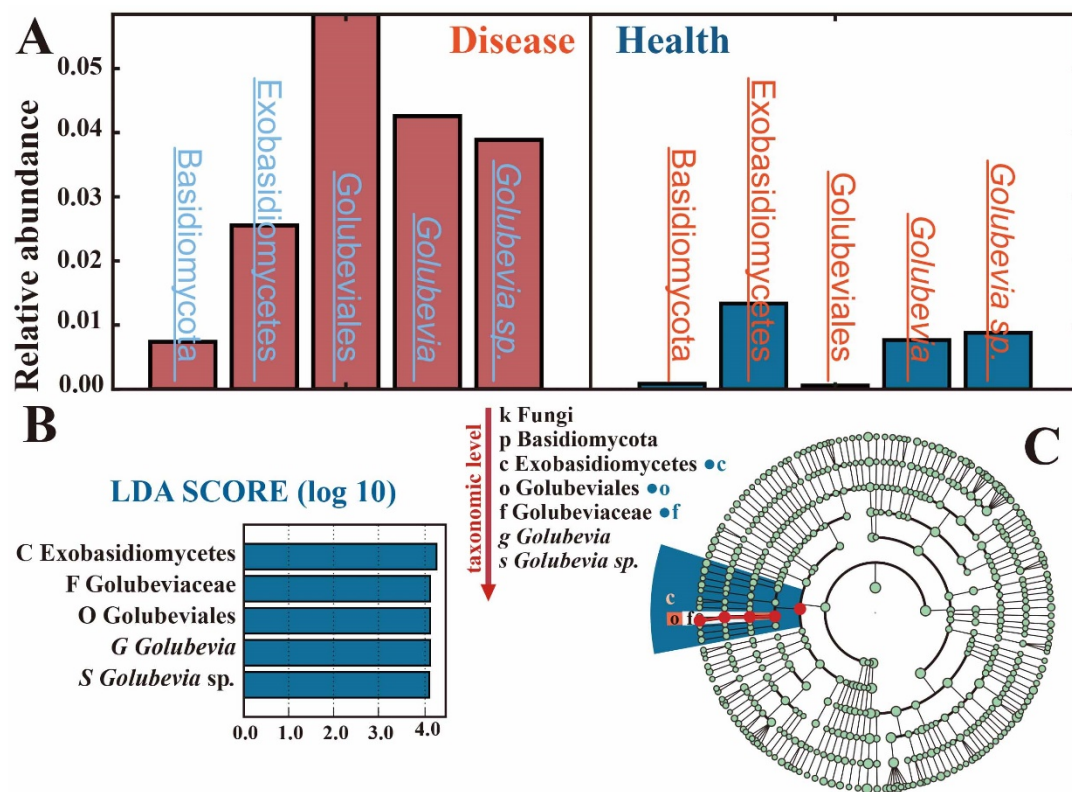


Figure 5. Biomarkers with statistically significant differences between healthy and diseased fruit searched by LDA Effect Size (LEfSe). **(A)** Comparison of relative abundance of biomarkers between groups. **(B)** A histogram of the distribution of LDA values. The LDA value distribution histogram shows the species whose LDA Score is greater than the set value, that is the biomarker with statistically significant differences between groups. The length of the histogram represents the influence of different species (LDA Score). **(C)** Cladogram of the biomarkers. Biomarkers with statistically significant differences between diseased and healthy tissue groups were searched with LDA Effect Size (LEfSe). LEfSe statistical results included a histogram of the distribution of LDA values, an evolutionary bifurcation (phylogenetic distribution), and a comparison of the abundance of biomarkers with statistically significant differences between diseased and healthy tissues groups. In the branching diagram, the circles radiating from the inside out represent the taxonomic level from the phylum to the species. Each small circle at a different classification level represents a classification at that level, and the diameter of the small circle is proportional to the relative abundance size. All species without significant differences were uniformly colored green, and the biomarker for differential species was stained in the following groups. The red nodes represent the microbial groups that play an important role in the pathogenesis group.

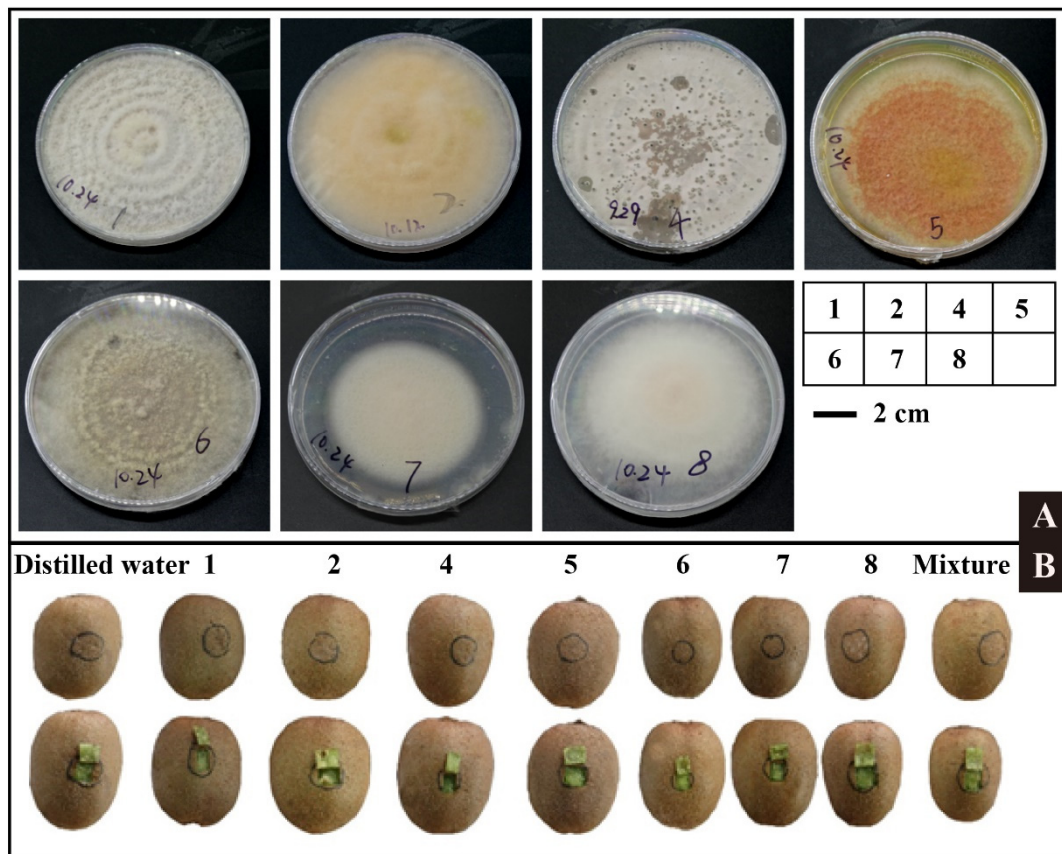


Figure 6. Isolation and inoculation of pathogenic fungus. (A) Isolation and purification of pathogenic fungi. (B) Observation on inoculation of pathogen from 'CuiXiang' fruit.

4. Conclusions

Black spot disease on kiwifruit is affecting the quality and profitability of postharvest production in Shaanxi province. We applied a high-throughput ITS sequencing method to the analysis of the black spot disease microbial community. The purpose of this study was to explore pathogenic fungal species of 'CuiXiang' kiwifruit black spot disease and to provide a basis for field prevention and treatment. The present study facilitated the illustration of disease mechanisms. In conclusion:

(1) Physiological, morphological and transcriptional characteristics between black spot fruit and healthy fruits were evaluated, and it was found that black spot can affect the ethylene production of healthy kiwifruit, which results in the firmness decreasing rapidly and the shelf life shortening. The results of the electron microscope show that black spots of kiwifruit were mainly distributed on the fruit surface, surface attached hyphae, and the number of starch granules and mitochondria decreased in kiwifruit with black spot disease, and transcriptome results showed that differential genes were involved in cell wall modification, pathogen perception, and signal transduction.

(2) There was a significant difference in fungal communities between healthy and diseased tissues. We analyzed key fungal species with differences between diseased and healthy fruits and predicted candidate pathogenic fungi included *Cladosporium cladosporioides*, *Diaporthe phaseolorum*, *Alternaria alternata*, and *Trichothecium roseum*, which have been reported to cause plant disease. Some species that were relatively abundant in healthy tissue have biological control effects in agricultural production, such as *Hanseniaspora uvarum*, *Acremonium sclerotigenum*, *Acaromyces ingoldii*, and *Aureobasidium pullulans*.

(3) A total of seven pathogens were isolated from harvested kiwifruit with disease infection. The results showed that single pathogen and mixed pathogen failed to show

black spots on the surface of the kiwifruit, which also showed that the formation of black spot disease was a complex process and needed more in-depth research.

This study described the microstructure of ‘CuiXiang’ kiwifruit black spot disease and identified potential pathogenic microorganisms by describing fungal diversity between healthy and diseased tissues. This study made a preliminary study on kiwifruit black spot, which can provide a reference for further research in the future.

Supplementary Materials: The following are available online at <https://www.mdpi.com/article/10.3390/horticulturae8010013/s1>. Figure S1: Inspection of the surface of ‘CuiXiang’ kiwifruit with different condition of black spot disease. Figure S2: Physicochemical properties of different severity of ‘CuiXiang’ kiwifruit black spot disease during storage. Table S1: Text mining results of pathogenicity of the significant fungi. Table S2: The lesion diameter of ‘CuiXiang’ kiwifruit inoculated with 7 kinds of fungi respectively.

Author Contributions: Data curation, L.C.; formal analysis, Y.Y. and L.C.; funding acquisition, Y.D.; investigation, C.W. and R.L.; methodology, Y.Y., H.P., C.W. and C.L.; project administration, W.Y.; resources, C.W.; software, H.P.; supervision, Y.D. and X.R.; validation, W.Y.; visualization, W.Y. and R.L.; writing—original draft, Y.Y. and L.C.; writing—review and editing, Y.Y. and L.C. All authors have read and agreed to the published version of the manuscript.

Funding: This work was supported by Primary Research and Development Plan of Ningxia Hui Autonomous Region (2021BBF0214); Introduction of Domestic Doctoral Programs in Shaanxi Province (16–18); and the Chinese Universities Scientific Fund (2452019018).

Institutional Review Board Statement: Not applicable.

Informed Consent Statement: Not applicable.

Data Availability Statement: The datasets presented in this study can be found in online repository of the NCBI Sequence Read Archive: <https://www.ncbi.nlm.nih.gov/bioproject/PRJNA673939/> (accessed on 19 December 2021).

Conflicts of Interest: The authors declare that there are no conflict of interest regarding the publication of this article.

References

1. Qi, X.; Guo, D.; Wang, R.; Zhong, Y.; Fang, J. Development status and suggestions on Chinese ki-wifruit industry. *J. Fruit Sci.* **2020**, *37*, 754–763.
2. Liu, Q.; Guo, Y.; He, P. Current Situation, Problems and Countermeasures of Kiwifruit Industry in China. *Guizhou Agric. Sci.* **2020**, *48*, 69–73.
3. Hirsch, A.-M.; Longeon, A.; Guyot, M. Fraxin and esculin: Two coumarins specific to *Actinidia chinensis* and *A. deliciosa* (kiwifruit). *Biochem. Syst. Ecol.* **2002**, *30*, 55–60. [[CrossRef](#)]
4. Jin, P. Formation reason and prevention and control measures of black spot in Cuixiang Kiwifruit fruit. *Northwest Hortic. (Fruit Trees)* **2015**, *5*, 26–28.
5. Yang, T.; Meng, J.; Chen, C. Kiwifruit ‘CuiXiang’ black spot prevention and control. *J. Shanxi Fruit Trees* **2019**, *3*, 84–86.
6. Fu, B.; Wang, J.; Ren, P.; Li, Y.; Zhao, J.; Jin, P.; Zhang, F. Identification of the pathogen causing black spot on kiwifruit in Shaanxi Province. *Acta Phytopathol. Sin.* **2020**, *50*, 112–116.
7. Wang, X.; Zhao, L.; Wang, B.; Li, L.; Zhang, Y. Prevention and control technology of black spot of Cuixiang ki-wifruit. *Shaanxi Agric. Sci.* **2016**, *62*, 125–126.
8. Pan, H.; Chen, M.Y.; Deng, L.; Wang, Z.P.; Li, L.; Zhong, C.H. First Report of *Didymella glomerata* Causing Black Spot Disease of Kiwifruit in China. *Plant Dis.* **2018**, *102*, 2654. [[CrossRef](#)]
9. Li, L.; Pan, H.; Chen, M.Y.; Zhang, S.J.; Zhong, C.H. First Report of *Nigrospora oryzae* Causing Brown/Black Spot Disease of Kiwifruit in China. *Plant Dis.* **2018**, *102*, 243. [[CrossRef](#)]
10. Kwon, J.-H.; Cheon, M.-G.; Kim, J.-W.; Kwack, Y.-B. Black Rot of Kiwifruit Caused by *Alternaria alternata* in Korea. *Plant Pathol. J.* **2011**, *27*, 298. [[CrossRef](#)]
11. Kikuhara, K.; Nakashima, C. Sooty spot of kiwifruit caused by *Pseudocercospora actinidiae* Deighton. *J. Gen. Plant Pathol.* **2008**, *74*, 185–187. [[CrossRef](#)]
12. Zhang, Z.; Guo, C.; Wang, Y.; Zhen, X. Identification and ITS Sequence Analysis of Gerbera Root Rot Pathogen. *Plant Pathol. Bull.* **2005**, *5*, 392–396.
13. Yuan, Y.; Li, J.; Lin, S.; Jia, H.; Pan, Y.; Luo, H.; Deng, M. Study on microbial diversity and function prediction of Pekinensis bean juice based on 16S rDNA high-throughput sequencing technology. *Food Ind. Sci. Technol.* **2020**, *41*, 95–100.

14. Janisiewicz, W.J.; Ii, W.M.J.; Peter, K.A.; Kurtzman, C.P.; Buyer, J. Yeasts associated with plums and their potential for controlling brown rot after harvest. *Yeast* **2014**, *31*, 207–218. [[CrossRef](#)]
15. Abdelfattah, A.; Wisniewski, M.; Droby, S.; Schena, L. Spatial and compositional variation in the fungal communities of organic and conventionally grown apple fruit at the consumer point-of-purchase. *Hortic. Res.* **2016**, *3*, 16047. [[CrossRef](#)]
16. Volschenk, Q.; Du Plessis, E.M.; Duvenage, F.J.; Korsten, L. Effect of postharvest practices on the culturable filamentous fungi and yeast microbiota associated with the pear carpoplane. *Postharvest Biol. Technol.* **2016**, *118*, 87–95. [[CrossRef](#)]
17. Li, L.; Pan, H.; Chen, M.; Zhang, S.; Zhong, C. Isolation and identification of pathogenic fungi causing postharvest fruit rot of kiwifruit (*Actinidia chinensis*) in China. *J. Phytopathol.* **2017**, *165*, 782–790. [[CrossRef](#)]
18. Barboni, T.; Cannac, M.; Chiaramonti, N. Effect of cold storage and ozone treatment on physicochemical parameters, soluble sugars and organic acids in *Actinidia deliciosa*. *Food Chem.* **2010**, *121*, 946–951. [[CrossRef](#)]
19. Park, Y.S.; Polovka, M.; Suhaj, M.; Ham, K.-S.; Kang, S.G.; Park, Y.-K.; Arancibia-Avila, P.; Toledo, F.; Sánchez, M.R.; Gorinstein, S. The postharvest performance of kiwi fruit after long cold storage. *Eur. Food Res. Technol.* **2015**, *241*, 601–613. [[CrossRef](#)]
20. Shahkoomahally, S.; Chaparro, J.X.; Beckman, T.G.; Sarkhosh, A. Influence of Rootstocks on Leaf Mineral Content in the Subtropical Peach cv. UFSun. *Am. Soc. Hortic. Sci.* **2020**, *55*, 496–502. [[CrossRef](#)]
21. da Silva, J.S.; Lavorante, A.F.; Paim, A.P.S.; da Silva, M.J. Microwave-assisted digestion employing diluted nitric acid for mineral determination in rice by ICP OES. *Food Chem.* **2020**, *319*, 8. [[CrossRef](#)]
22. Rahman, M.U.; Ma, Q.; Ahmad, B.; Hanif, M.; Zhang, Y. Histochemical and Microscopic Studies Predict that Grapevine Genotype “Ju mei gui” is Highly Resistant against *Botrytis cinerea*. *Pathogens* **2020**, *9*, 253. [[CrossRef](#)]
23. Lopez Velasco, G.; Tydings, H.A.; Boyer, R.R.; Falkinham, J.O., III; Ponder, M.A. Characterization of interactions between *Escherichia coli* O157:H7 with epiphytic bacteria in vitro and on spinach leaf surfaces—ScienceDirect. *Int. J. Food Microbiol.* **2012**, *153*, 351–357. [[CrossRef](#)] [[PubMed](#)]
24. Zhang, L.; Wang, S. Bacterial community diversity on in-shell walnut surfaces from six representative provinces in China. *Sci. Rep.* **2017**, *7*, 10054. [[CrossRef](#)]
25. Edgar, R.C.; Haas, B.J.; Clemente, J.C.; Quince, C. UCHIME improves sensitivity and speed of chimera detection. *Bioinformatics* **2011**, *27*, 2194–2200. [[CrossRef](#)]
26. Edgar, R.C. UPARSE: Highly accurate OTU sequences from microbial amplicon reads. *Nat. Methods* **2013**, *10*, 996–998. [[CrossRef](#)] [[PubMed](#)]
27. White, J.R.; Nagarajan, N.; Pop, M. Statistical Methods for Detecting Differentially Abundant Features in Clinical Metagenomic Samples. *PLoS Comput. Biol.* **2009**, *5*, e1000352. [[CrossRef](#)]
28. Santoni, F.; Paolini, J.; Barboni, T.; Costa, J. Relationships between the leaf and fruit mineral compositions of *Actinidia deliciosa* var. Hayward according to nitrogen and potassium fertilization. *Food Chem.* **2013**, *147*, 269–271. [[CrossRef](#)] [[PubMed](#)]
29. Kumarihami, H.; Cha, G.H.; Kim, J.G.; Kim, H.U.; Lee, M.; Kwack, Y.B.; Cho, J.G.; Kim, J. Effect of Preharvest Ca-chitosan Application on Postharvest Quality of ‘Garmrok’ Kiwifruit during Cold Storage. *Hortic. Sci. Technol.* **2020**, *38*, 239–248.
30. Veraverbeke, E.; Verboven, P.; van Oostveldt, P.; Nicolai, B. Prediction of moisture loss across the cuticle of apple (*Malus sylvestris* subsp. *mitis* (Wallr.)) during storage: Part 2. Model simulations and practical applications. *Postharvest Biol. Technol.* **2003**, *30*, 75–88. [[CrossRef](#)]
31. Gilbert, H.J. The Biochemistry and Structural Biology of Plant Cell Wall Deconstruction. *Plant Physiol.* **2010**, *153*, 444–455. [[CrossRef](#)]
32. Zhang, B.; Chen, K.; Bowen, J.; Allan, A.; Espley, R.; Karunairetnam, S.; Ferguson, I. Differential expression within the LOX gene family in ripening kiwifruit. *J. Exp. Bot.* **2006**, *57*, 3825–3836. [[CrossRef](#)]
33. Wang, Y.; Xiong, G.; He, Z.; Yan, M.; Zou, M.; Jiang, J. Transcriptome analysis of *Actinidia chinensis* in response to *Botrytis dothidea* infection. *PLoS ONE* **2020**, *15*, e0227303.
34. Haile, Z.M.; Guzman, N.D.; Grace, E.; Moretto, M.; Sonogo, P.; Engelen, K.; Zoli, L.; Moser, C.; Baraldi, E. Transcriptome Profiles of Strawberry (*Fragaria vesca*) Fruit Interacting with *Botrytis cinerea* at Different Ripening Stages. *Front. Plant Sci.* **2019**, *10*, 1131. [[CrossRef](#)]
35. Liu, H.; Guo, J.; Cheng, Y.; Liu, P.; Long, C.; Deng, B. Inhibitory activity of tea polyphenol and *Hanseniaspora uvarum* against *Botrytis cinerea* infections. *Lett. Appl. Microbiol.* **2010**, *51*, 258–263. [[CrossRef](#)] [[PubMed](#)]
36. Parish, M.; Beuchat, L.; Suslow, T.; Harris, L.; Garrett, E.; Farber, J.; Busta, F. Methods to Reduce/Eliminate Pathogens from Fresh and Fresh-Cut Produce. *Compr. Rev. Food Sci. Food Saf.* **2003**, *2*, 161–173. [[CrossRef](#)]
37. Chen, J.; Yan, R.; Hu, Y.; Zhang, N.; Hu, H. Compositional shifts in the fungal diversity of garlic scapes during postharvest transportation and cold storage. *LWT* **2019**, *115*, 108453. [[CrossRef](#)]
38. Ghule, S.B.; Sawant, I.S.; Sawant, S.D.; Saha, S.; Devarumath, R.M. Isolation and identification of three new mycoparasites of *Erysiphe necator* for biological control of grapevine powdery mildew. *Australas. Plant Pathol.* **2019**, *48*, 351–367. [[CrossRef](#)]
39. Liu, H.M.; Guo, J.H.; Cheng, Y.J.; Li, L.; Pu, L.; Wang, B.Q.; Deng, B.X.; Long, C.A. Control of gray mold of grape by *Hanseniaspora uvarum* and its effects on postharvest quality parameters. *Ann. Microbiol.* **2010**, *60*, 31–35. [[CrossRef](#)]
40. Di Francesco, A.; Di Foggia, M.; Corbetta, M.; Baldo, D.; Ratti, C.; Baraldi, E. Biocontrol Activity and Plant Growth Promotion Exerted by *Aureobasidium pullulans* Strains. *J. Plant Growth Regul.* **2020**, *40*, 1233–1244. [[CrossRef](#)]